Journal of Hydrology 570 (2019) 445–453

Contents lists available at ScienceDirect

Journal of Hydrology

journal homepage: www.elsevier.com/locate/jhydrol

Research papers

Stable isotope ratios of typhoon rains in Fuzhou, Southeast China, during 2013–2017

Tao Xu[a], Xiaoshuang Sun[a], Hui Hong[a], Xiaoyan Wang[a], Mengyue Cui[a], Guoliang Lei[a,b], Lu Gao[a,b], Juan Liu[c,*], Mahjoor Ahmad Lone[d,e], Xiuyang Jiang[a,b,*]

[a] Key Laboratory for Humid Subtropical Eco-geographical Process of the Ministry of Education, School of Geographical Sciences, Fujian Normal University, Fuzhou 350007, China
[b] Institute of Geography, Fujian Normal University, Fuzhou 350007, China
[c] Innovation Center and Key Laboratory of Waters Safety & Protection in the Pearl River Delta, Ministry of Education, Guangzhou University, Guangzhou 510006, China
[d] High-Precision Mass Spectrometry and Environment Change Laboratory (HISPEC), Department of Geosciences, National Taiwan University, Taipei 106, Taiwan, ROC
[e] Research Center for Future Earth, National Taiwan University, Taipei 10617, Taiwan, ROC

ARTICLE INFO

This manuscript was handled by Huaming Guo, Editor-in-Chief, with the assistance of Philippe Negrel, Associate Editor

Keywords:
Typhoon
Rainfall
Stable isotope ratios
Southeast China
Rain shield effect

ABSTRACT

Stable isotope ratios (δ^2H and $\delta^{18}O$) in precipitation not only show a certain response to climate change at different time scales, but also have strong linkages to extreme weather events such as tropical cyclones (hurricanes/typhoons). Typhoon activity in the coastal region of Southeast China is quite intense, bringing huge amounts of moisture; thus, contributing to extreme rainfall in this region. The existing isotope data in Southeast China is available on a monthly or daily temporal resolution, which is inadequate to study 1–2-day-long typhoon rainfall events at a particular location. In this study, hourly rainfall δ^2H and $\delta^{18}O$ data are collected for eight typhoon events from 2013 to 2017 in Fuzhou, Southeast China. The total correlation between δ^2H and $\delta^{18}O$ is obtained as $\delta^2H = 7.41\ \delta^{18}O + 0.81$ ($R^2 = 0.96$, $N = 220$). All the eight typhoon events reveal a similar variability pattern in $\delta^{18}O$ values which can be divided into three stages. More positive $\delta^{18}O$ values occur in the first and third stages, while the second stage is dominated by most negative $\delta^{18}O$ values, exhibiting an inverted U-shaped pattern. The positive $\delta^{18}O$ values during the first and third stages are governed by re-evaporation. The precipitation during the second stage has distinctly lower $\delta^{18}O$ values than the weighted average $\delta^{18}O$ of summer precipitation in Fuzhou. Some of these values are slightly lower than those of the water vapor over the Pacific Ocean's surface. No significant relationship is observed between precipitation $\delta^{18}O$ and temperature as well as the amount of precipitation during the second stage. We hypothesize that the significant ^{18}O-depletion is mainly caused by the 'rain shield effect', which refers to combination of large-scale convection, high condensation efficiency, and recycling of isotopically depleted vapor in rain shield areas leading to very negative $\delta^{18}O$ values during typhoon system. These findings suggest the use of stable isotope ratios as important tracers of typhoon water.

1. Introduction

As an important part of the global water cycle, stable isotopes in modern precipitation contain rich climatic and environmental information (e.g., Araguás-Araguás et al., 2000; Xie et al., 2011; Ren et al., 2017). Stable hydrogen and oxygen isotopes (δ^2H and $\delta^{18}O$) in precipitation have been widely used in studies pertaining to the hydrological cycle and climatology (e.g., Tian et al., 2007; Yao et al., 2013; Brenčič et al., 2015; Srivastava et al., 2015). Since 1961, the International Atomic Energy Agency (IAEA) and the World Meteorological Organization (WMO) established the Global Network of Isotopes in Precipitation (GNIP) program to survey stable isotopes in worldwide precipitation. The acquired data have greatly improved our knowledge of isotopic compositions in precipitation and their response to environmental changes (e.g., Gat, 1996; Bowen and Wilkinson, 2002; Vuille et al., 2005). A notable positive correlation between δ^2H and $\delta^{18}O$ is called Meteoric Water Line (MWL), and can be observed in precipitations, lakes, and rivers around the world. The Global Meteoric Water Line (GMWL) is given as $\delta^2H = 8\ \delta^{18}O + 10$ (Craig, 1961), and plays an important role in the study of stable isotopes in precipitation

* Corresponding authors at: School of Geographical Sciences, Fujian Normal University, Fuzhou 350007, China (X. Jiang) and Guangzhou University, Guangzhou 510006, China (J. Liu).
E-mail addresses: liujuan858585@163.com (J. Liu), xyjiang@fjnu.edu.cn (X. Jiang).

https://doi.org/10.1016/j.jhydrol.2019.01.017
Received 16 November 2018; Received in revised form 4 January 2019; Accepted 8 January 2019
Available online 18 January 2019

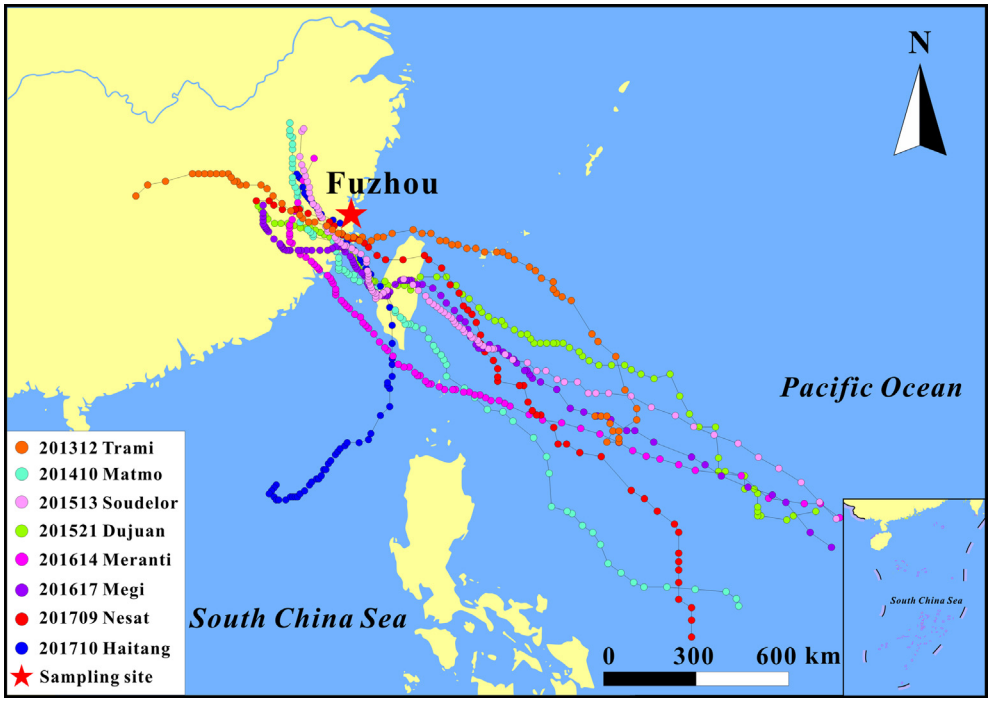

Fig. 1. The paths of eight typhoons and location of typhoon precipitation samples collected in Fuzhou (red star), Southeast China, from 2013 to 2017. (For interpretation of the references to colour in this figure legend, the reader is referred to the web version of this article.)

(Araguás-Araguás et al., 1998; Tian et al., 2001; Zhou and Li, 2017). The apparent correlations between stable hydrogen and oxygen isotopes in precipitation and meteorological and geographical parameters are known as isotope effects, and include the temperature, amount, altitude, and latitude effects (Dansgaard, 1964). Among them, the temperature effect and the amount effect are particularly important (Dansgaard, 1964; Siegenthaler and Oeschger, 1980; Baldini et al., 2010). Previous studies have found that change in the sources of water vapor also has an important impact on stable isotope ratios in precipitation (Hoffmann and Heimann, 1997; Breitenbach et al., 2010; Peng et al., 2010; Chen and Li, 2018). Considerable research has been conducted on stable isotope ratios in precipitation on monthly and daily basis in different regions of the world (e.g., Gammons et al., 2006; Liu et al., 2010; Stumpp et al., 2014; Zhang and Wang, 2016). However, the precise relationship between stable isotopic compositions and meteorological parameters during extreme precipitation events remain controversial. In some cases, the variation of isotope compositions during the extreme rainfall event is also attributed to change in moisture sources (Xie et al., 2011; Li et al., 2015).

In general, heavy precipitation caused by extreme weather, such as torrential rain or tropical cyclones, is categorized as an extreme precipitation event. Tropical cyclones are characterized by strong wind, high-intensity precipitation, and a wide range of impacts (Zhang et al., 2018). The stable isotope compositions of precipitation in tropical cyclones could be used as tracers of the storm structure, dynamic evolution, and its water and energy budgets (Lawrence et al., 1982, 2002; Lawrence and Gedzelman, 1996; Good et al., 2014; Munksgaard et al., 2015). The mean $\delta^{18}O$ values in hurricane precipitations are obviously lower than those of other tropical and summer precipitation systems, and the isotope ratios decrease inward toward the center of the hurricane (Lawrence and Gedzelman, 1996; Gedzelman et al., 2003). Lawrence et al. (1998) explained that the low stable isotope ratios in hurricanes result from their high and deep clouds, large size, and longevity, and the inward decrease is due to isotope exchange between precipitation and depleted vapor in the atmospheric boundary layer. While studying the Typhoon Shanshan, similar results were found by Fudeyasu et al. (2008), who attributed this low stable isotope ratio to the rainout effect. Ohsawa and Yusa (2000) suggested that the stable isotope ratios decrease with the reduction of distance between the typhoon and observation site, and this phenomenon is related to the isotopic fractionation of water vapor. Therefore, a clear understanding of the short-term isotopic variability of tropical cyclones is fundamental in interpreting precipitation isotopes in tropical and subtropical regions.

The coastal area of South China is especially vulnerable to landfalling typhoons from the western North Pacific (Zhang et al., 2009, 2011). Typhoons bring abundant water vapor from the ocean and provide favorable environments for the initiation of extreme precipitation in the coastal and landward regions of China (Zhang et al., 2018). Typhoon activity in Southeast China is very intense during summer and autumn. One of the regions with the largest number of landfalling typhoons in China is Fujian Province (Zhang et al., 2009). From May 2000 to October 2017, Fujian Province experienced 141 typhoons, of which 42 made landfall. Owing to the changes in the environment and the underlying surface, the structure, path, and intensity of typhoons change significantly during the process of moving and making landfall on the mainland (Chen et al., 2010). Thus, understanding this variability and the fundamental causes behind it are important to interpret the hydrological cycle during typhoon events. Stable isotopes in precipitation have been broadly utilized in hydrological and meteorological studies (Hoefs, 2015; He et al., 2018a). Thus, clarifying the variations in the characteristics of typhoon precipitation $\delta^{18}O$ and the influencing factors during its occurrence are of great significance. The existing monthly precipitation isotopic data in southern China are presented by GNIP while daily records are generated by Xie et al. (2011) and Chen et al. (2016). Since, the impact of typhoon precipitation lasts for only 1–2 days at a particular location, the existing stable isotope data is inadequate for intra-event comparison.

In this study, we report hourly precipitation $\delta^{2}H$ and $\delta^{18}O$ collected during eight typhoon events from 2013 to 2017 in Fuzhou, Southeast China. The major objectives are (1) to investigate the intra-event variability of precipitation stable isotopes during typhoon events; (2) to examine the influence of meteorological parameters at the sampling site

on precipitation stable isotopes; and (3) to explore the factors impacting significant ^{18}O-depletion in the rain during typhoon events.

2. Sampling site

The precipitation samples were collected at the top of a ~20 m high building that hosts the School of Geographical Sciences in Fujian Normal University (26°05′ N, 119°30′ E; 31 m a.s.l.). The sampling site is located in Fuzhou, which is in the lower reaches of the Minjiang River in Southeast China, next to the Taiwan Strait (Fig. 1). Fuzhou is typically dominated by a subtropical monsoon climate. It has hot and rainy summers, and warm and dry winters. Instrumental meteorological data from the Fuzhou meteorological station (1981–2010; 26°08′ N, 119°28′ E; 84 m a.s.l.) shows that the average annual temperature is 20 °C and the average annual precipitation is 1390 mm. The monthly average maximum and minimum temperature is 29 °C and 11 °C, occurring in July and January, respectively. More than 80% of average annual precipitation is concentrated in the rainy season from March to September (Supplementary Fig. S1). Typhoon activities in the area mainly occur from June to September (JJAS), with ~1–2 typhoons affect or make landfall every year. The amount of precipitation during typhoon usually account for 50%–80% of the monthly precipitation during summer monsoon (JJAS) and 6%–17% of the annual precipitation.

3. Materials and methods

From 2013 to 2017, eight typhoon events had a significant impact on Fuzhou (Fig. 1). Among them, seven typhoons originated from the western North Pacific and the remaining one originated from the South China Sea (Fig. 1 and Table 1). During their respective development, four of them reached the lifetime maximum intensity of a "Super Typhoon," two others were classified as "Typhoon," while the remaining two typhoons were categorized as "Strong Typhoon" and "Tropical Storm" (Table 1 and Supplementary Table S1). The total accumulated precipitation during each of these typhoons range from 50 mm to 300 mm during the entire sampling period (Table 1). More details about eight typhoons are given in Supplementary Text S1.

Owing to changes in precipitation amounts, the samples of typhoon precipitation were collected at different time intervals (0.5 h–2 h). A clean 2-L glass beaker was used to collect the typhoon precipitation. The beaker was placed on a shelf about 1.5 m above ground, and packed with tinfoil. A funnel was placed on top of the beaker to prevent evaporation. Once the sampling was completed, each sample was immediately poured into 50-mL and 2-mL polypropylene colorless plastic bottles with no air headspace. These bottles were sealed with Parafilm sealing membrane to prevent evaporation and stored in a refrigerator at 4 °C to avoid isotopic fractionation until stable isotopic analysis could be performed. A total of 220 samples were collected during the 8 typhoons.

Stable isotope compositions (δ^2H and $\delta^{18}O$) of the samples were measured using LGR DLT-100 Liquid Water Isotope Analyzer (Los Gatos Research, Inc., Mountain View, CA, USA). This analysis was conducted at the Nanjing Institute of Geography and Limnology, Chinese Academy of Sciences, China. Calibration of the measurements used four internal standards ($\delta^{18}O$: −2.80‰, −7.69‰, −13.10‰, and −16.14‰; δ^2H: −9.5‰, −51.0‰, −96.4‰, and −123.6‰). The results of the stable isotope compositions are expressed as δ-values, relative to the standard V-SMOW (Vienna Standard Mean Ocean Water); δ (‰) = $(R_{sample} - R_{standard})/R_{standard} \times 1000$, where R refers to the $^{18}O/^{16}O$ or $^2H/^1H$ ratio. The measurement accuracy was typically ± 0.5‰ for δ^2H and ± 0.1‰ for $\delta^{18}O$.

The hourly meteorological parameters (surface air temperature, precipitation amount, and relative humidity) during the sampling period and historical meteorological data (1981–2010) at Fuzhou meteorological station were downloaded from http://www.weather.com.cn and http://data.cma.cn. The δ^2H and $\delta^{18}O$ of precipitation in Fuzhou station (1985–1992; 26°08′ N, 119°28′ E; 16 m a.s.l.) were obtained from the GNIP website at https://nucleus.iaea.org/wiser.

4. Results

4.1. The range and evolution of stable isotopes during typhoon events

Descriptive statistics of δ^2H and $\delta^{18}O$ of typhoon precipitation in Fuzhou from 2013 to 2017, together with GNIP based monthly precipitation δ^2H and $\delta^{18}O$ from 1985 to 1992 are presented in Table 1. The δ^2H and $\delta^{18}O$ values of all typhoon precipitation samples vary greatly from −10‰ to −122‰ and from −2.6‰ to −17‰, respectively (Table 1 and Supplementary Table S2). The GNIP based monthly precipitation δ^2H and $\delta^{18}O$ ranges from 1‰ to −104.7‰ and from −0.92‰ to −14.16‰, respectively (Table 1). Both δ^2H and $\delta^{18}O$ of all typhoon events exhibit larger amplitude than monthly precipitation.

GNIP based weighted mean precipitation $\delta^{18}O$ value during summer (JJAS) between 1985 and 1992 is −8.1‰ (Table 1). Marking this $\delta^{18}O$ (−8.1‰) as the background value, the characteristics of typhoon precipitation $\delta^{18}O$ over the entire events are divided into three stages (Figs. 2 and S2). The $\delta^{18}O$ values are generally positive during the first stage (−2.6‰ to −9.9‰), followed by a significant decrease during the second stage (−6.3‰ to −17‰), while the third stage is marked with a gradual increase (−3.3‰ to −10.7‰). During the first and

Table 1
Descriptive statistics of precipitation δ^2H and $\delta^{18}O$ in Fuzhou.

	Lifetime maximum intensity	P (mm)	Origin area		δ^2H (‰)			$\delta^{18}O$ (‰)		
			Lon (°/E)	Lat (°/N)	Max	Min	Mean	Max	Min	Mean
Trami (2013)	Typhoon	72.5	127.6	20.9	−45	−118	−101	−5.3	−16	−13.2
Matmo (2014)	Strong Typhoon	172.5	135.2	10.2	−49	−117	−97	−7.2	−15.4	−12.9
Soudelor (2015)	Super Typhoon	314	159.2	13.6	−10	−85	−59	−3.2	−11.4	−8.2
Dujuan (2015)	Super Typhoon	124	138.2	17.7	−17	−110	−53	−2.6	−15	−7.4
Meranti (2016)	Super Typhoon	60	139.1	14.9	−37	−119	−88	−5.4	−16	−12.1
Megi (2016)	Super Typhoon	306.5	140.1	15.6	−25	−110	−64	−3	−13.6	−8.8
Nesat (2017)	Typhoon	56.5	127.9	15.7	−37	−102	−85	−2.6	−15.5	−11.2
Haitang (2017)	Tropical Storm	145	115.6	18.5	−37	−122	−80	−5.3	−17	−11.3
GNIP (1985–1992)					1	−104.7	−41.3	−0.92	−14.16	−6.4
$GNIP_{JJAS}$ (1985–1992)					−14.1	−84	−58.7	−0.92	−11.78	−8.1

P means the total precipitation amount of each typhoon event.
The mean δ-values of typhoon precipitation are averaged by hourly precipitation amount, using the equation $\delta = \sum_{i=1}^{n} P_i\delta_i / \sum_{i=1}^{n} P_i$, where P_i and δ_i denote hourly precipitation and its δ value.
The mean δ-values of GNIP are averaged by monthly precipitation amount, using the equation $\delta = \sum_{i=1}^{n} P_i\delta_i / \sum_{i=1}^{n} P_i$, where P_i and δ_i denote monthly precipitation and its δ value.

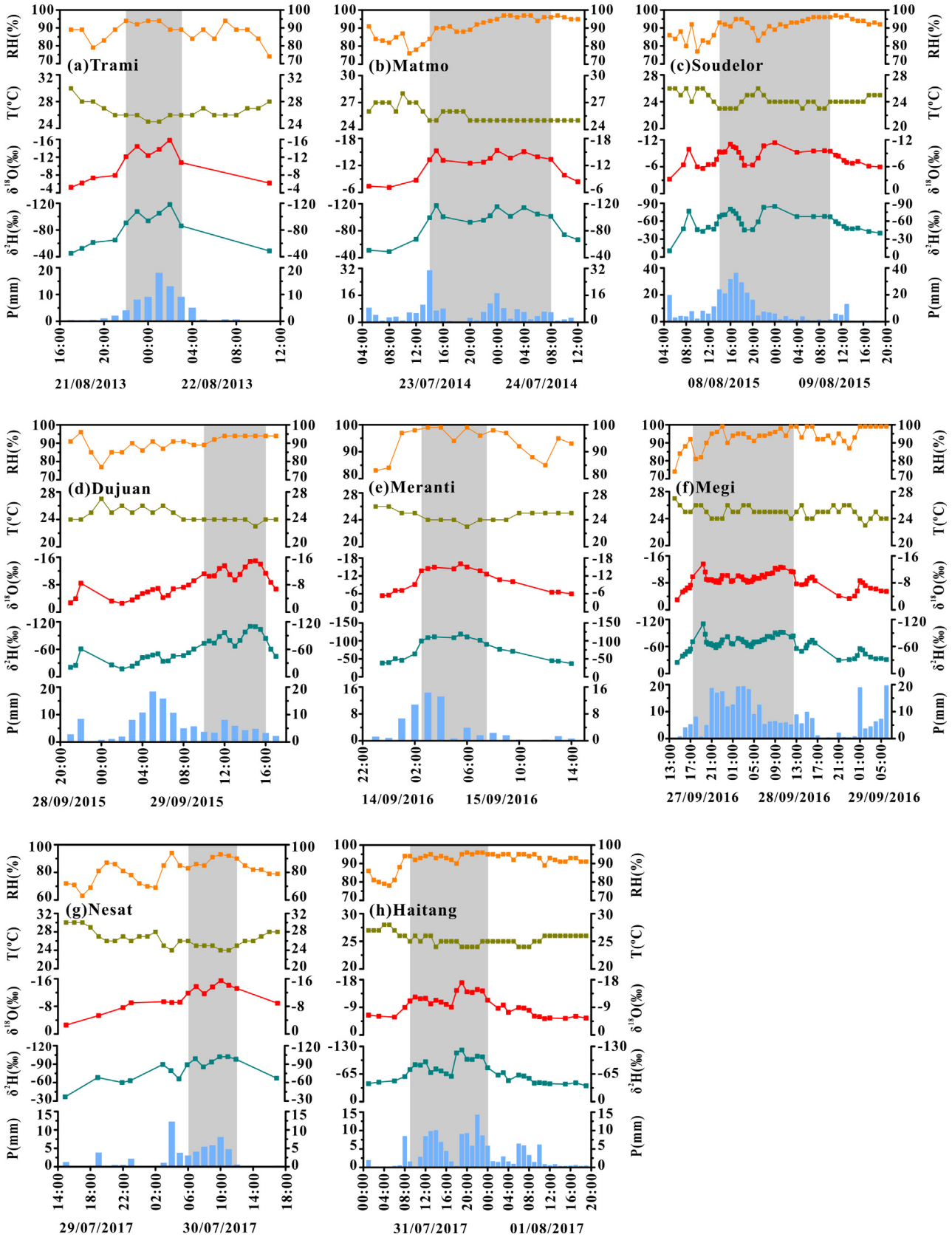

Fig. 2. Stage characteristics of δ^2H (dark cyan), $\delta^{18}O$ (red) and meteorological parameters, including relative humidity (RH, orange), air temperature (T, dark yellow) and precipitation amount (P, blue) in Fuzhou. (a) Typhoon Trami (201312); (b) Typhoon Matmo (201410); (c) Typhoon Soudelor (201513); (d) Typhoon Dujuan (201521); (e) Typhoon Meranti (201614); (f) Typhoon Megi (201617); (g) Typhoon Nesat (201709); (h) Typhoon Haitang (201710). The format of sampling time all belong to China Standard Time UT + 8:00 (CST). The shaded bars indicate the second stage of each typhoon precipitation process. (For interpretation of the references to colour in this figure legend, the reader is referred to the web version of this article.)

third stages, the relatively enriched $\delta^{18}O$ values show wide fluctuations while the excessively negative $\delta^{18}O$ values during the second stage are relatively steady. The variation in $\delta^{18}O$ in the process of typhoon precipitation shows an inverted U-shaped pattern (Fig. 2).

4.2. Inter-event variability

Significant variation in $\delta^{2}H$ and $\delta^{18}O$ values of the precipitation is also observed within each typhoon event. Typhoon Dujuan (2015) and Typhoon Nesat (2017) reveals the largest range for $\delta^{2}H$ (−17‰ to −110‰) and $\delta^{18}O$ (−2.6‰ to −15.5‰), respectively. However, Typhoon Nesat (2017) show the smallest range for $\delta^{2}H$ (−37‰ to −102‰), while Typhoon Matmo (2014) and Typhoon Soudelor (2015) show the smallest range for $\delta^{18}O$ (−7.2‰ to −15.4‰ and −3.2‰ to −11.4‰), respectively (Table 1). Nevertheless, there is a minimal difference in the lowest precipitation $\delta^{2}H$ and $\delta^{18}O$ values between the typhoon events, which ranges from −102‰ to −122‰ and −13.6‰ to −17‰, respectively (Table 1). Although, Typhoon Soudelor (2015) is an exception as it shows relatively enriched values of $\delta^{2}H$ and $\delta^{18}O$ (−85‰ and −11.4‰), respectively.

The weighted mean $\delta^{2}H$ and $\delta^{18}O$ values during typhoon events and monthly precipitation also vary considerably. Typhoon Dujuan (2015) and Typhoon Trami (2013) show the largest and smallest weighted mean values for both $\delta^{2}H$ (−53‰ and −101‰) and $\delta^{18}O$ (−7.4‰ and −13.2‰), respectively. GNIP based $\delta^{2}H$ and $\delta^{18}O$ values during summer (JJAS) ranges from −14.1‰ to −84‰ and from −0.92‰ to −11.78‰ respectively, and the weighted mean values are −58.7‰ and −8.1‰, respectively (Table 1). The most negative $\delta^{2}H$ and $\delta^{18}O$ values in typhoon precipitation are significantly lower than those of the monthly precipitation events in Fuzhou, which is probably because the GNIP datasets are weighed by monthly average precipitation to provide a comprehensive picture. The $\delta^{18}O$ values of a total of 137 typhoon precipitation samples (~62% of the total number of typhoon precipitation samples) are lower than −8.1‰.

4.3. Correlation analysis between stable isotopes and meteorological parameters

Correlations between local meteorological parameters (air temperature, precipitation amount, and relative humidity) and $\delta^{18}O$ of typhoon precipitation for different time periods are given in Table 2. During the entire sampling period, the first and third stages, there is a weak positive correlation between temperature and $\delta^{18}O$, and a weak negative correlation between relative humidity and $\delta^{18}O$ (Table 2). The correlation coefficient (r) are 0.33 ($p < 0.01$, $n = 171$), 0.30 ($p < 0.01$, $n = 85$) between $\delta^{18}O$ and temperature, and −0.33 ($p < 0.01$, $n = 171$), −0.24 ($p < 0.05$, $n = 85$) between $\delta^{18}O$ and relative humidity during the entire period, and the first and third stages, respectively. There is no apparent correlation between meteorological parameters and precipitation $\delta^{18}O$ for the second stage (Table 2). The correlations between $\delta^{18}O$ and meteorological parameters suggest that stable isotopes of typhoon precipitation are not controlled by local meteorological variables on the ground. The temperature and relative humidity recorded by the rain gauge or meteorological station can only partially represent the atmospheric conditions below the clouds (He et al., 2018b). However, variability in these data can also provide some insights to explain the isotopic evolution pattern (e.g., higher temperature and lower relative humidity may imply a higher re-evaporation).

Table 2
Statistics of correlations between meteorological parameters and $\delta^{18}O$ in typhoon precipitation over three different timescales.

Meteorological parameters	Sampling period	Second stage	First and third stages
	$\delta^{18}O$	$\delta^{18}O$	$\delta^{18}O$
T	0.33** (171)	0.05 (86)	0.30** (85)
P	−0.18* (171)	0.21 (86)	−0.05 (85)
RH	−0.33** (171)	−0.16 (86)	−0.24* (85)

T means air temperature, P means precipitation amount, RH means relative humidity.
** Correlation is significant at the 0.01 level (2-tailed).
* Correlation is significant at the 0.05 level (2-tailed).

4.4. Deuterium excess (d-excess)

Deuterium excess (d-excess), defined as $d = \delta^{2}H - 8 \times \delta^{18}O$, is generally controlled by evaporative conditions combining sea surface temperature, humidity, and wind speed (Dansgaard, 1964; Merlivat and Jouzel, 1979; Benetti et al., 2014). d-excess values of typhoon precipitation also observed to vary greatly through time, from 21.9‰ to −25.5‰ (Fig. S3). More than 80% of the total number of typhoon precipitation samples shows d-excess value of less than 10‰. The mean d-excess value is 6.3‰. Unlike $\delta^{18}O$, d-excess values exhibit irregular variability with no inverted U-shaped variability. With the raindrops fall below the cloud, it can be affected by sub-cloud evaporation, which increases ^{18}O and decreases deuterium excess (Hollins et al., 2018). There is an inverse relationship existing between $\delta^{18}O$ and d-excess values ($r = -0.4$, $p < 0.01$), suggesting the occurrence of re-evaporation to some extent of raindrops during typhoon events (He et al., 2018b).

5. Discussion

5.1. Correlation between $\delta^{2}H$ and $\delta^{18}O$ in typhoon precipitation

The MWL of typhoon precipitation in Fuzhou is presented as $\delta^{2}H = 7.41\ \delta^{18}O + 0.81$ ($R^2 = 0.96$, $N = 220$). Both the slope and intercept are slightly smaller than those of the GMWL ($\delta^{2}H = 8\ \delta^{18}O + 10$; Craig, 1961) and the LMWL ($\delta^{2}H = 8.84\ \delta^{18}O + 16.94$, $R^2 = 0.96$, $N = 48$) (Fig. 3). The LMWL is established from the $\delta^{2}H$ and $\delta^{18}O$ values of Fuzhou station as per GNIP data from January 1988 to December 1991. Previous studies suggest that the degree of precipitation re-evaporation is likely associated with the relative humidity conditions in different environments (Lee and Fung, 2008; He et al., 2018b). Before and after typhoon landfall, the relative humidity is low, ranging from 63% to 95%. More than 50% of these values are lower

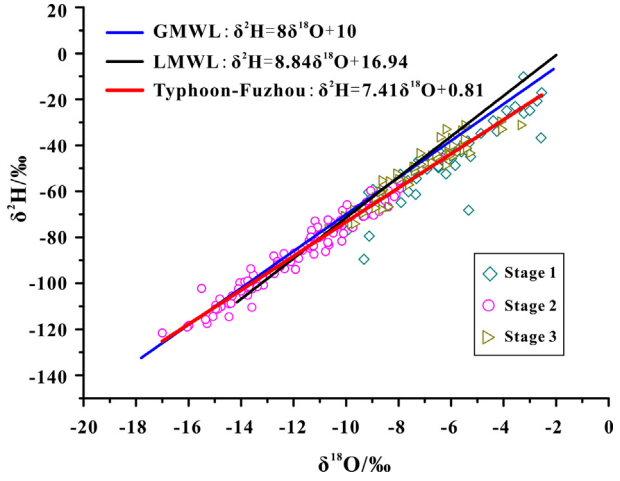

Fig. 3. Correlation between $\delta^{2}H$ and $\delta^{18}O$ in the typhoon precipitation of Fuzhou. The regression line for typhoon precipitation, the Global Meteoric Water Line (GMWL), and the Local Meteoric Water Line (LMWL) of Fuzhou are presented for comparison.

than 90%. The $\delta^{18}O$ values of typhoon precipitation are relatively enriched (> −8‰) and appears in the lower right of the GMWL and LMWL plots (Fig. 3). Previously analysis suggests that Southeast China is strongly affected by the western North Pacific subtropical high in summer (Lin and Wang, 2016). Water vapor evaporates to some extent before and after typhoon landfall, which usually results in heavy isotope enrichment of typhoon precipitation and the relatively enriched precipitation $\delta^{18}O$ values due to the isotopic non-equilibrium fractionation. The rain shield area of a typhoon affects the sampling site, increasing relative humidity to ~100%. The $\delta^{18}O$ values of typhoon precipitation are significantly negative (< −8‰) and plot closely to the GMWL and the LMWL (Fig. 3), which indicates very weak re-evaporation of precipitation during this period. The effect of re-evaporation before and after typhoon landfall leads to smaller slope and intercept of the MWL of typhoon precipitation in Fuzhou compared to the corresponding values of the GMWL and LMWL.

5.2. Stage characteristics of $\delta^{18}O$

The first stage shows relatively enriched $\delta^{18}O$ values ranging from −2.6‰ to −9.9‰, with a weighted mean of −6.5‰ (Fig. 2). During a typhoon, re-evaporation has the greatest impact at the initial stage of precipitation as the vapor content in the air is lower (Muller et al., 2015). Precipitation during this stage is mainly influenced by the water vapor in the periphery of rain shield, and is characterized by higher temperature, less precipitation amount, and lower relative humidity (Fig. 2). When the typhoon approaches the sampling site (Supplementary Fig. S2), the precipitation $\delta^{18}O$ values gradually become negative (Fig. 2).

During the second stage, the $\delta^{18}O$ values vary from −6.3‰ to −17‰, with a weighted mean of ~ −12‰ (Fig. 2). More than 80% of the $\delta^{18}O$ values range from −9‰ to −17‰, and 30% of these values are even lower than the original $\delta^{18}O$ value of water vapor in the clouds (~ −13‰; Siegenthaler, 1979). Only four relatively enriched $\delta^{18}O$ values exceeded −8.1‰ for Typhoon Soudelor (2015), which may be attributed to the changes in meteorological conditions. The temperature drops slightly as the $\delta^{18}O$ value decreases and is maintained at 24 °C to 26 °C (Fig. 2). Precipitation during this stage is mainly influenced by the rain shield area of the typhoon. The precipitation accounts for 70%–90% of the total amount during each typhoon with an exception of Typhoon Dujuan (2015), where it sums up for only 30%. Moreover, the average relative humidity is more than 90% during this stage (Fig. 2). Furthermore, the $\delta^{18}O$ values are significantly negative, remaining relatively steady with smaller fluctuations as compared to the other two stages.

During the third stage, the $\delta^{18}O$ values vary from −3.3‰ to −10.7‰, with a weighted mean of −7.3‰ (Fig. 2). As the typhoon moves longer distance away from our sampling site (Supplementary Fig. S2), the precipitation amount decreases and the mean $\delta^{18}O$ value increases gradually with time. However, the mean $\delta^{18}O$ value is still relatively lower than the first stage, which may be related to the third stage precipitation that is partially influenced by the depletion of heavy isotope in the residual water vapor of the second stage.

Overall, the precipitation $\delta^{18}O$ variability in each typhoon is characterized by three stages (Fig. 2). These stage characteristics are independent of source regions (the western North Pacific and the South China Sea). Our results indicate that change in moisture sources may exert a negligible influence on the $\delta^{18}O$. Previous studies suggest no significant difference in seawater $\delta^{18}O$ and surface temperature between the tropical oceans (LeGrande and Schmidt, 2006; Cai et al., 2017; He et al., 2018a). The consistent inverted U-shaped pattern in $\delta^{18}O$ variability despite different sources likely implies similar microphysical processes governing the general evolution of precipitation $\delta^{18}O$ during typhoons.

In addition to the stage characteristics, the variation in $\delta^{18}O$ values in typhoon precipitation also shows a spatial structure. As shown in Fig. 4, variation characteristics of the $\delta^{18}O$ values correspond well with the distance between the typhoon center and the sampling site (Lawrence and Gedzelman, 1996; Ohsawa and Yusa, 2000; Gedzelman et al., 2003; Fudeyasu et al., 2008). As the distance decreases, the values of precipitation $\delta^{18}O$ during eight typhoons gets more negative ($r = 0.4$, and $p < 0.01$), and the most negative values generally occur within 20 km–300 km range. Typhoon Haitang (2017) is an exception because some of the lowest $\delta^{18}O$ values occur beyond 300 km (Fig. 4). This typhoon originated in the northern part of the South China Sea, and its precipitation process got concentrated mainly after the landfall in the mainland (Fig. 2). Although the typhoon center is located away from Fuzhou, the sampling site continues to experience rain due to the effects of the residual water vapor. Therefore, some of the most negative $\delta^{18}O$ values for Typhoon Haitang (2017) occur beyond 300 km.

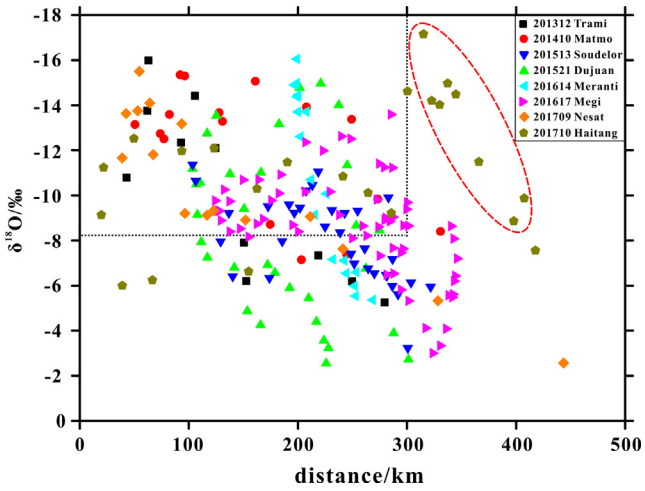

Fig. 4. Relationship between the $\delta^{18}O$ in typhoon precipitation and the distance between the typhoon center and the sampling site. The black dotted lines represent the $\delta^{18}O$ values in typhoon precipitation are lower than −8.1‰ and within 300 km. The red dash line marked some of the $\delta^{18}O$ values for Typhoon Haitang (201710) are lower than −8.1‰ but occur beyond 300 km. (For interpretation of the references to colour in this figure legend, the reader is referred to the web version of this article.)

5.3. Rain shield effect of $\delta^{18}O$ in typhoon precipitation

Based on the correlation analysis between $\delta^{18}O$ and meteorological parameters, it is observed that stable isotopes of typhoon precipitation are not controlled by local meteorological variables on the ground. Therefore, we attempt to understand this phenomenon via two perspectives viz., (1) oxygen isotopic fractionation and (2) the microphysical process of the typhoon system.

The classic Rayleigh fractionation pattern of precipitation (Siegenthaler, 1979) indicates that the initial $\delta^{18}O$ value in sea water is ~0‰ (Fig. 5a). When sea water evaporates, the lighter ^{16}O is concentrated in the water vapor, and thus, the $\delta^{18}O$ value of the water vapor in clouds is more negative. Using the fractionation factors (1.0793 and 1.00937 for $\delta^{2}H$ and $\delta^{18}O$, respectively) of water evaporation from ocean surface under isotope equilibrium fractionation conditions at 25 °C (Majoube, 1971), the $\delta^{2}H$ and $\delta^{18}O$ values are calculated to be −79‰ and −9.4‰, respectively (Lawrence et al., 2004). However, the evaporation in a natural environment occurs mostly under non-equilibrium fractionation conditions. Thus, the actual $\delta^{18}O$ value of water vapor is more negative than the $\delta^{18}O$ value under equilibrium fractionation (~ −13‰; Fig. 5a). For instance, Craig and Gordon (1965) found that the initial $\delta^{18}O$ values of the water vapor over the North Pacific Ocean ranges from −10.5‰ to −14‰. When water vapor is transported to the mainland, the heavier ^{18}O will drop preferentially during the condensation and precipitation processes. The

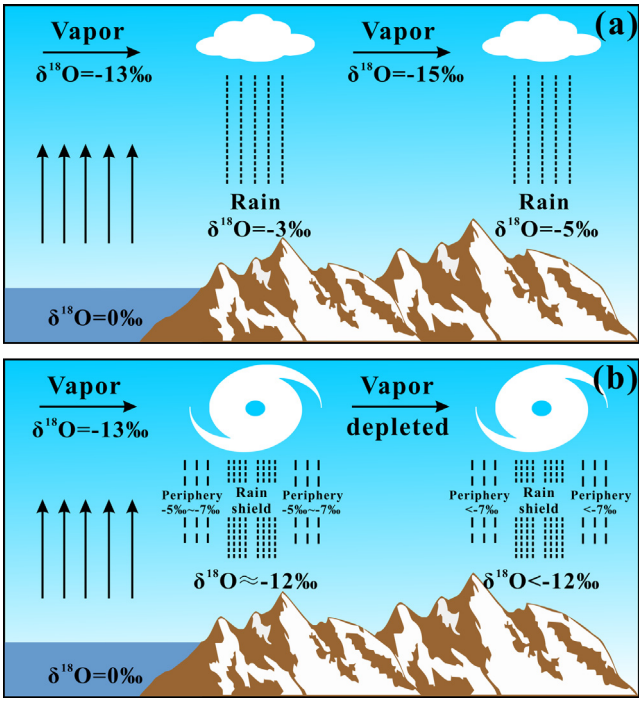

Fig. 5. Oxygen isotopic fractionation patterns (a) precipitation event (b) typhoon precipitation event.

earliest precipitation $\delta^{18}O$ value is relatively enriched (~ −3‰; Fig. 5a). It is close to that of the ocean water and usually represents the first portion of condensate from undisturbed ocean moisture (Darling et al., 2006). As water vapor moves inland and continues to form precipitation, the residual water vapor gets increasingly depleted in ^{18}O, and the $\delta^{18}O$ value of water vapor in clouds is more negative (~ −15‰; Fig. 5a). With the process of continuous precipitation, stable isotopes are affected by temperature, amount, latitude, and continental effects. Therefore, the $\delta^{18}O$ value of precipitation gradually becomes further negative (~ −5‰; Fig. 5a). This observation is consistent with a previous study by Liu et al. (2008) which suggests average annual precipitation $\delta^{18}O$ value in Southeast China at ~ −5‰ to −7‰.

Southeast China is strongly affected by the western North Pacific subtropical high during summer (Lin and Wang, 2016). Thus, the vapor content of the air is lower, and the initial stage of precipitation tends to re-evaporate (Muller et al., 2015). When the periphery of rain shield approaches the sampling site, re-evaporation enriches the mean $\delta^{18}O$ values of precipitation, ranging from −5‰ to −7‰ (Fig. 5b). However, the precipitation $\delta^{18}O$ values during the second stage of typhoon events are extremely negative, ranging from −6.3‰ to −17‰ (Fig. 2), with a mean value is ~ −12‰ (Fig. 5b). Some of these values are slightly above that of the water vapor over the Pacific Ocean surface. Therefore, it can't be interpreted by the classic Rayleigh fractionation pattern. We hypothesize that the extremely negative $\delta^{18}O$ values during the second stage of typhoon precipitation are mainly caused by the 'rain shield effect'.

Typhoons include a highly efficient precipitation system. As shown in Fig. 2, the precipitation accounts for 70%–90% of the total amount, and the average relative humidity is more than 90% during the second stage. Typhoons are characterized by intense large-scale convective activity and strong cyclonic circulation, specifically in the eye wall and spiral rain bands. Greatest wind speeds and heaviest rainfall always occur in these regions (Lutgens and Tarbuck, 2013). During the convective updraft, water vapor rapidly condenses and raindrops fall in a saturated environment (Fig. 6). The high condensation efficiency of rainstorms could lead to extremely negative precipitation $\delta^{18}O$ values (Lawrence and Gedzelman, 1996). Convective clouds not only have rotational and deep intense updrafts, but tend to have relatively weak downdrafts (Houze, 2010). As shown in Fig. 6, the isotopically depleted remnant vapor after the condensation reaches the sub-cloud layer and towards the typhoon center along with the downdrafts. Typhoon is fueled by the latent heat when huge quantities of vapor condense (Lutgens and Tarbuck, 2013). Therefore, a large quantity of warm, moist vapor is continuously supplied from the ocean surface (Fig. 6). As the inward rush of surface vapor approaches the center of the typhoon, it turns upward. The isotopically depleted vapor is also taken up into the subsequent convective condensation process (Risi et al., 2008, 2010; Kurita, 2013; Lekshmy et al., 2014; Munksgaard et al., 2015). This successive convective condensation and precipitation cycles make the isotopic compositions of precipitation and vapor more depleted. Hence, recycling of isotopically depleted vapor also plays an important role in the rain ^{18}O depletion during the typhoon system. In conclusion, combination of large-scale convection, high condensation efficiency, and recycling of isotopically depleted vapor in rain shield areas leading to very negative $\delta^{18}O$ values during typhoon system.

As the typhoon makes landfall in the land, the supply of ocean surface vapor is cut off (Lutgens and Tarbuck, 2013). As a consequence, the recycling of isotopically depleted vapor ceases. When the typhoon moves inland and forms precipitation, even in some regions farther away from the landfall area, the $\delta^{18}O$ values also become increasingly negative (Fig. 5b). This result is consistent with the classic Rayleigh fractionation pattern of precipitation. The results of precipitation $\delta^{18}O$ for Typhoon Nesat (2017), collected in Fuzhou and Sanming (~150 km

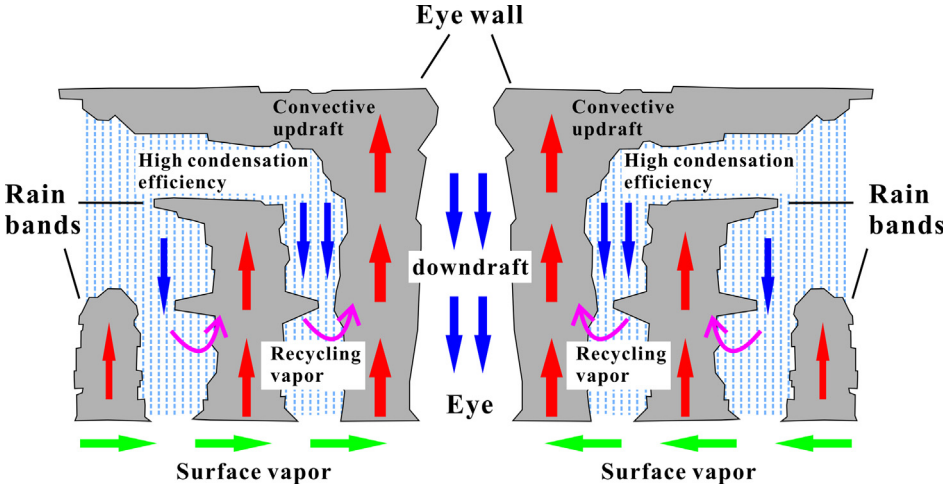

Fig. 6. Schematic diagrams of the microphysical process in the typhoon system (cross section).

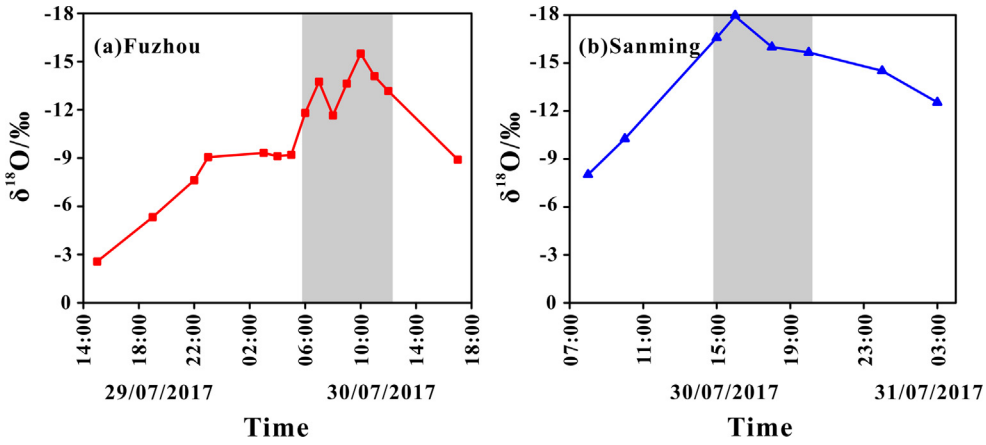

Fig. 7. Stage characteristics of the precipitation $\delta^{18}O$ of Typhoon Nesat (201709) in (a) Fuzhou and (b) Sanming. The shaded bars indicate the second stage of typhoon precipitation process.

west of Fuzhou) (Supplementary Fig. S4), show that the $\delta^{18}O$ values in Fuzhou and Sanming vary from −2.6‰ to −15.5‰ and from −8‰ to −17.9‰, respectively (Fig. 7 and Supplementary Table S2). During the second stage in Sanming, the $\delta^{18}O$ values vary from −15.7‰ to −17.9‰, and the weighted mean $\delta^{18}O$ is −17‰, which is significantly lower than the weighted average $\delta^{18}O$ value of −13.7‰ during the second stage of typhoon precipitation in Fuzhou. The mean $\delta^{18}O$ values during the first and third stages in Sanming also become more negative than those for Fuzhou (Fig. 7). As the typhoon moves inland, preferable removal of heavy isotopes during the successive condensation causes a general shift towards depleted precipitation $\delta^{18}O$ from the coastal (Fuzhou) to the inland areas (Sanming) (Fig. 5b).

6. Conclusions

This study presents the results of hourly stable isotope compositions (δ^2H and $\delta^{18}O$) in precipitation collected from eight typhoons from 2013 to 2017 in Fuzhou, Southeast China. The δ^2H and $\delta^{18}O$ values of all typhoon precipitation samples vary greatly from −10‰ to −122‰ and from −2.6‰ to −17‰, respectively. The most negative δ^2H and $\delta^{18}O$ values in typhoon precipitation are significantly lower than those of the monthly precipitation events.

The MWL of typhoon precipitation is presented as $\delta^2H = 7.41\ \delta^{18}O + 0.81$ ($R^2 = 0.96$, $N = 220$), and the slope and intercept are slightly smaller than those of the GMWL and the LMWL. The analysis suggests significant re-evaporation of precipitation during, before, and after typhoon landfall, resulting in heavy isotope enrichment in typhoon precipitation. This leads to the smaller slope and intercept of the MWL for typhoon precipitation compared to those of the GMWL and LMWL.

The characteristics of $\delta^{18}O$ variability during the entire process of typhoon precipitation can be divided into three stages. Relatively enriched $\delta^{18}O$ values occur in the first and third stages, while significantly negative $\delta^{18}O$ values occur in the second stage, showing an inverted U-shaped pattern. Southeast China is strongly affected by the western North Pacific subtropical high during summer, the positive $\delta^{18}O$ values for typhoon precipitation during the first and third stages are governed by re-evaporation. There is no significant correlation between typhoon precipitation $\delta^{18}O$ and meteorological parameters (air temperature, precipitation amount, and relative humidity) during the second stage. This finding also demonstrates that the extremely negative $\delta^{18}O$ values during the second stage are not controlled by local meteorological variables. We hypothesize that the most negative $\delta^{18}O$ values during the second stage are mainly caused by the 'rain shield effect'. That is, combination of large-scale convection, high condensation efficiency, and recycling of isotopically depleted vapor in rain shield areas leading to very negative $\delta^{18}O$ values during typhoon system.

Declaration of interest

None.

Acknowledgements

This study was jointly supported by grants of the National Key Research and Development Program of China (2017YFA0603401), the National Natural Science Foundation of China (41672170), the Program for New Century Excellent Talents in Fujian Province University, the Program for Innovative Research Team of Fujian Normal University (IRTL1705), and the Guangzhou University's 2017 training program for young top-notch personnel (BJ201709).

Appendix A. Supplementary data

Supplementary data to this article can be found online at https://doi.org/10.1016/j.jhydrol.2019.01.017.

References

Araguás-Araguás, L., Froehlich, K., Rozanski, K., 1998. Stable isotope composition of precipitation over southeast Asia. J. Geophys. Res. 103 (D22), 28721–28742.
Araguás-Araguás, L., Froehlich, K., Rozanski, K., 2000. Deuterium and oxygen-18 isotope composition of precipitation and atmospheric moisture. Hydrol. Process. 14 (8), 1341–1355.
Baldini, L.M., McDermott, F., Baldini, J.U., Fischer, M.J., Möllhoff, M., 2010. An investigation of the controls on Irish precipitation $\delta^{18}O$ values on monthly and event timescales. Clim. Dyn. 35 (6), 977–993.
Benetti, M., Reverdin, G., Pierre, C., Merlivat, L., Risi, C., Steen-Larsen, H.C., Vimeux, F., 2014. Deuterium excess in marine water vapor: dependency on relative humidity and surface wind speed during evaporation. J. Geophys. Res. 119 (2), 584–593.
Bowen, G.J., Wilkinson, B., 2002. Spatial distribution of $\delta^{18}O$ in meteoric precipitation. Geology 30 (4), 315–318.
Breitenbach, S.F.M., Adkins, J.F., Meyer, H., Marwan, N., Kumar, K.K., Haug, G.H., 2010. Strong influence of water vapor source dynamics on stable isotopes in precipitation observed in Southern Meghalaya, NE India. Earth. Planet. Sci. Lett. 292 (1), 212–220.
Brenčič, M., Kononova, N.K., Vreča, P., 2015. Relation between isotopic composition of precipitation and atmospheric circulation patterns. J. Hydrol. 529 (3), 1422–1432.
Cai, Z.Y., Tian, L.D., Bowen, G.J., 2017. ENSO variability reflected in precipitation oxygen isotopes across the Asian Summer Monsoon region. Earth. Planet. Sci. Lett. 475, 25–33.
Chen, Y.T., Du, W.J., Chen, J.S., Xu, L.L., 2016. Composition of hydrogen and oxygen isotopic of precipitation and source apportionment of water vapor in Xiamen area. Acta Sci. Circum. 36 (2), 667–674 (in Chinese with English abstract).
Chen, L.S., Li, Y., Cheng, Z.Q., 2010. An overview of research and forecasting on rainfall associated with landfalling tropical cyclones. Adv. Atmos. Sci. 27 (5), 967–976.
Chen, C.J., Li, T.Y., 2018. Geochemical characteristics of cave drip water respond to ENSO based on a 6-year monitoring work in Yangkou Cave, Southwest China. J. Hydrol. 561, 896–907.
Craig, H., 1961. Isotopic variation in meteoric waters. Science 133 (3465), 1702–1703.
Craig, H., Gordon, L.I., 1965. Deuterium and oxygen 18 variations in the ocean and the

marine atmosphere. In: Tongiorgi, E. (Ed.), Stable Isotopes in Oceanographic Studies and Paleotemperatures. Lischi and Figli, Pisa, Italy, pp. 9–130.
Dansgaard, W., 1964. Stable isotopes in precipitations. Tellus 16 (4), 436–468.
Darling, W.G., Bath, A.H., Gibson, J.J., Rozanski, K., 2006. Isotopes in water. In: Leng, M.J. (Ed.), Isotopes in Paleoenvironmental Research. Springer, Dordrecht, pp. 1–66.
Fudeyasu, H., Ichiyanagi, K., Sugimoto, A., Yoshimura, K., Ueta, A., Yamanaka, M.D., Ozawa, K., 2008. Isotope ratios of precipitation and water vapor observed in Typhoon Shanshan. J. Geophys. Res. 113, (D12113). https://doi.org/10.1029/2007JD009313.
Gammons, C.H., Poulson, S.R., Pellicori, D.A., Reed, P.J., Roesler, A.J., Petrescu, E.M., 2006. The hydrogen and oxygen isotopic composition of precipitation, evaporated mine water, and river water in Montana, USA. J. Hydrol. 328 (1–2), 319–330.
Gat, J.R., 1996. Oxygen and hydrogen isotopes in the hydrologic cycle. Annu. Rev. Earth Planet. Sci. 24 (1), 225–262.
Gedzelman, S., Lawrence, J., Gamache, J., Black, M., Hindman, E., Black, R., Dunion, J., Willoughby, H., Zhang, X., 2003. Probing hurricanes with stable isotopes of rain and water vapor. Mon. Weather. Rev. 131 (6), 1112–1127.
Good, S.P., Mallia, D.V., Lin, J.C., Bowen, G.J., 2014. Stable isotope analysis of precipitation samples obtained via crowdsourcing reveals the spatiotemporal evolution of Superstorm Sandy. PLoS One 9 (3), e91117. https://doi.org/10.1371/journal.pone.0091117.
He, S.N., Goodkin, N.F., Jackisch, D., Ong, M.R., Samanta, D., 2018a. Continuous real-time analysis of the isotopic composition of precipitation during tropical rain events: Insights into tropical convection. Hydrol. Process. 32 (11), 1531–1545.
He, S.N., Goodkin, N.F., Kurita, N., Wang, X.F., Rubin, C.M., 2018b. Stable isotopes of precipitation during tropical Sumatra squalls in Singapore. J. Geophys. Res. 123, 3812–3829.
Hoefs, J., 2015. Stable Isotope Geochemistry, seventh ed. Springer, Switzerland.
Hoffmann, G., Heimann, M., 1997. Water isotope modeling in the Asian monsoon region. Quat. Int. 37 (2), 115–128.
Hollins, S.E., Hughes, C.E., Crawford, J., Cendón, D.I., Meredith, K.T., 2018. Rainfall isotope variations over the Australian continent–implications for hydrology and isoscape applications. Sci. Total. Environ. 645, 630–645.
Houze, R.A., 2010. Clouds in tropical cyclones. Mon. Weather. Rev. 138 (2), 293–344.
Kurita, N., 2013. Water isotopic variability in response to mesoscale convective system over the tropical ocean. J. Geophys. Res. 118 (18), 10376–10390.
Lawrence, J.R., Gedzelman, S.D., White, J.W.C., Smiley, D., Lazov, P., 1982. Storm trajectories in eastern US D/H isotopic composition of precipitation. Nature 296 (5858), 638–640.
Lawrence, J.R., Gedzelman, S.D., 1996. Low stable isotope ratios of tropical cyclone rains. Geophys. Res. Lett. 23 (5), 527–530.
Lawrence, J.R., Gedzelman, S.D., Zhang, X.P., Arnold, R., 1998. Stable isotope ratios of rain and vapor in 1995 hurricanes. J. Geophys. Res. 103 (D10), 11381–11400.
Lawrence, J.R., Gedzelman, S.D., Gamache, J., Black, M., 2002. Stable isotope ratios: Hurricane Olivia. J. Atmos. Chem. 41 (1), 67–82.
Lawrence, J.R., Gedzelman, S.D., Dexheimer, D., Cho, H.K., Carrie, G.D., Gasparini, R., Anderson, C.R., Bowman, K.P., Biggerstaff, M.I., 2004. Stable isotopic composition of water vapor in the tropics. J. Geophys. Res. 109, (D06115). https://doi.org/10.1029/2003JD004046.
Lee, J.E., Fung, I., 2008. "Amount effect" of water isotopes and quantitative analysis of post-condensation processes. Hydrol. Process. 22 (1), 1–8.
Legrande, A.N., Schmidt, G.A., 2006. Global gridded data set of the oxygen isotopic composition in seawater. Geophys. Res. Lett. 33 (12), L12604. https://doi.org/10.1029/2006GL026011.
Lekshmy, P.R., Midhun, M., Ramesh, R., Jani, R.A., 2014. ^{18}O depletion in monsoon rain relates to large scale organized convection rather than the amount of rainfall. Sci. Rep. 4, 5661. https://doi.org/10.1038/srep05661.
Li, J., Tao, T., Pang, Z.H., Tan, M., Kong, Y.L., Duan, W.H., Zhang, Y.W., 2015. Identification of different moisture sources through isotopic monitoring during a storm event. J. Hydrometeorol. 16 (4), 1918–1927.
Lin, Z.D., Wang, B., 2016. Northern East Asian low and its impact on the interannual variation of East Asian summer rainfall. Clim. Dyn. 46 (1–2), 83–97.
Liu, J.R., Fu, G.B., Song, X.F., Charles, S.P., Zhang, Y.H., Han, D.M., Wang, S.Q., 2010. Stable isotopic compositions in Australian precipitation. J. Geophys. Res. 115, (D23307). https://doi.org/10.1029/2010JD014403.
Liu, Z.F., Tian, L.D., Chai, X.R., Yao, T.D., 2008. A model-based determination of spatial variation in precipitation $\delta^{18}O$ over China. Chem. Geol. 249 (1–2), 203–212.
Lutgens, F.K., Tarbuck, E.J., 2013. In: Hurricanes. The Atmosphere: An Introduction to Meteorology, 12th ed. Prentice Hall, NewYork, pp. 302–325.
Majoube, M., 1971. Fractionnement en oxygene 18 et en deuterium entre l'eau et sava-peur. J. Chim. Phys. 68, 1423–1436.
Merlivat, L., Jouzel, J., 1979. Global climate interpretation of the deuterium-oxygen 18 relationship for precipitation. J. Geophys. Res. 84 (C8), 5029–5033.
Muller, C.L., Baker, A., Fairchild, I.J., Kidd, C., Boomer, I., 2015. Intra-event trends in stable isotopes: exploring midlatitude precipitation using a vertically pointing micro rain radar. J. Hydrometeorol. 16, 194–213.
Munksgaard, N.C., Zwart, C., Kurita, N., Bass, A., Nott, J., Bird, M.I., 2015. Stable isotope anatomy of tropical cyclone Ita, North-Eastern Australia, April 2014. PLoS One 10 (3), e0119728. https://doi.org/10.1371/journal.pone.0119728.
Ohsawa, S., Yusa, Y., 2000. Isotopic characteristics of typhonic rainwater: typhoons no. 13 (1993) and no. 6 (1996). Limnology 1 (2), 143–149.
Peng, T.R., Wang, C.H., Huang, C.C., Fei, L.Y., Chen, C.T.A., Hwong, J.L., 2010. Stable isotopic characteristic of Taiwan's precipitation: a case study of western Pacific monsoon region. Earth. Planet. Sci. Lett. 289 (3–4), 357–366.
Ren, W., Yao, T.D., Xie, S.Y., He, Y., 2017. Controls on the stable isotopes in precipitation and surface waters across the southeastern Tibetan Plateau. J. Hydrol. 545, 276–287.
Risi, C., Bony, S., Vimeux, F., 2008. Influence of convective processes on the isotopic composition ($\delta^{18}O$ and δD) of precipitation and water vapor in the tropics: 2. Physical interpretation of the amount effect. J. Geophys. Res. 113, D19306. https://doi.org/10.1029/2008JD009943.
Risi, C., Bony, S., Vimeux, F., Chong, M., Descroix, L., 2010. Evolution of the stable water isotopic composition of the rain sampled along Sahelian squall lines. Q. J. R. Meteorol. Soc. 136 (S1), 227–242.
Siegenthaler, U., 1979. Stable hydrogen and oxygen isotopes in the water cycle. In: Jäger, E., Hunziker, J.C. (Eds.), Lectures in Isotope Geology. Springer, Berlin, Heidelberg, pp. 264–273.
Siegenthaler, U., Oeschger, H., 1980. Correlation of ^{18}O in precipitation with temperature and altitude. Nature 285 (5763), 314–317.
Srivastava, R., Ramesh, R., Gandhi, N., Jani, R.A., Singh, A.K., 2015. Monsoon onset signal in the stable oxygen and hydrogen isotope ratios of monsoon vapor. Atmos. Environ. 108, 117–124.
Stumpp, C., Klaus, J., Stichler, W., 2014. Analysis of long-term stable isotopic composition in German precipitation. J. Hydrol. 517 (4), 351–361.
Tian, L.D., Yao, T.D., Sun, W.Z., Stievenard, M., Jouzel, J., 2001. Relationship between δD and $\delta^{18}O$ in precipitation on north and south of the Tibetan Plateau and moisture recycling. Sci. China Ser. D Earth Sci. 44 (9), 789–796.
Tian, L.D., Yao, T.D., MacClune, K., White, J.W.C., Schilla, A., Vaughn, B., Vachon, R., Ichiyanagi, K., 2007. Stable isotopic variations in west China: a consideration of moisture sources. J. Geophys. Res. 112 (D10), D10112. https://doi.org/10.1029/2006JD007718.
Vuille, M., Werner, M., Bradley, R.S., Keimig, F., 2005. Stable isotopes in precipitation in the Asian monsoon region. J. Geophys. Res. 110, (D23108). https://doi.org/10.1029/2005JD006022.
Xie, L.H., Wei, G.J., Deng, W.F., Zhao, X.L., 2011. Daily $\delta^{18}O$ and δD of precipitations from 2007 to 2009 in Guangzhou, South China: implications for changes of moisture sources. J. Hydrol. 400 (3–4), 477–489.
Yao, T.D., Masson-Delmotte, V., Gao, J., Yu, W.S., Yang, X.X., Risi, C., Sturm, C., Werner, M., Zhao, H.B., He, Y., Ren, W., Tian, L.D., Shi, C.M., Hou, S.G., 2013. A review of climatic controls on $\delta^{18}O$ in precipitation over the Tibetan Plateau: observations and simulations. Rev. Geophys. 51 (4), 525–548.
Zhang, M.J., Wang, S.J., 2016. A review of precipitation isotope studies in China: basic pattern and hydrological process. J. Geog. Sci. 26 (7), 921–938.
Zhang, Q., Wu, L.G., Liu, Q.F., 2009. Tropical cyclone damages in China 1983–2006. B. Am. Meteorol. Soc. 90 (4), 489–495.
Zhang, Q., Zhang, W., Lu, X.Q., Chen, Y.D., 2011. Landfalling tropical cyclones activities in the south China: Intensifying or weakening? Int. J. Climatol. 32 (12), 1815–1824.
Zhang, Q., Gu, X.H., Li, J.F., Shi, P.J., Singh, V.P., 2018. The impact of tropical cyclones on extreme precipitation over coastal and inland areas of China and its association to ENSO. J. Climate. 31 (5), 1865–1880.
Zhou, J.L., Li, T.Y., 2017. A tentative study of the relationship between annual $\delta^{18}O$ & δD variations of precipitation and atmospheric circulations—a case from Southwest China. Quat. Int. 479, 117–127.